J|A|C|S COMMUNICATIONS

Published on Web 03/03/2010

Enhanced Stability of Gold Clusters Supported on Hydroxylated MgO(001) Surfaces

Matthew A. Brown, Esther Carrasco, Martin Sterrer,* and Hans-Joachim Freund

Department of Chemical Physics, Fritz-Haber-Institut der Max-Planck-Gesellschaft, D-14195 Berlin, Germany

Received January 14, 2010; E-mail: sterrer@fhi-berlin.mpg.de

While the microscopic details of CO oxidation over oxide-supported Au clusters remain debated in the literature, there exists general agreement that the size of the particles substantially affects catalytic performance. Au clusters less than 5 nm in diameter are needed for high catalytic activity in CO oxidation.[1,2] Sintering of Au clusters caused by thermal pretreatment or during reaction is a common cause in the loss of catalytic activity.[2,3] Therefore, understanding the role of the oxide support interface in stabilizing small Au clusters is fundamental to our understanding of heterogeneous surface reactions on supported Au catalysts.

The nucleation behavior of metals on single crystalline oxide supports has been studied extensively.[4] Previous ultrahigh vacuum (UHV) studies in our laboratory combined with theoretical calculations were successful in describing the bonding of gold atoms and the influence of point defects on the nucleation behavior of gold on clean, ideally terminated MgO(001) surfaces.[5] Under realistic conditions oxide surfaces usually exhibit a certain concentration of functional groups (e.g., hydroxyls and carbonates) that may influence the stability of metal clusters or may even be involved in the catalytic reaction.[6,7] In this respect it is interesting to note that high conversion in low-temperature CO oxidation was reported for Au supported on metal hydroxides such as $Mg(OH)_2$ and $Fe(OH)_x$.[8,9] These systems were found to stabilize subnanometer-sized gold particles and to have lost their catalytic activity after transformation into the oxide by thermal treatment, which also leads to Au particle sintering.

Surface science studies within a controlled environment are promising to yield a fundamental understanding regarding differences in metal nucleation and sintering properties on both perfect and more realistic oxide surfaces.[10] From UHV studies of Au nucleation on slightly reduced as well as mildly hydroxylated TiO_2(110) surfaces it was concluded that adsorption of water leads to enhanced agglomeration of Au particles caused by depletion of oxygen vacancy sites otherwise acting as nucleation centers.[11,12] In the work presented here, the nucleation of gold clusters on perfect MgO(001) as well as hydroxylated MgO(001) (MgO_{hydr}, $\theta(OH) \approx 0.4$ ML) surfaces is compared by spectroscopic methods using thin MgO(001) films supported on Ag(001). We show that surface modification by hydroxylation acts to limit sintering of Au particles at temperatures frequently employed to activate supported Au catalysts, thereby helping to maintain highly dispersed small Au clusters.

Figure 1 shows the CO TPD spectra from 0.5 Å Au deposited at 90 K onto (a) MgO(001) and (b) MgO_{hydr} for different annealing temperatures. CO bound to low coordinated (LC) sites on MgO is indicated by CO desorption at ~100 K.[13] The process of hydroxylation/dehydroxylation may lead to changes in the morphology of the surface and the reduced adsorption capacity on LC sites of MgO_{hydr} in the 90 and 300 K spectra (Figure 1b) reflects LC sites being quenched by OH. The CO peak desorption temperature from the freshly deposited Au particles is 180−185 K for both samples and results from CO bound to LC sites on the Au particles.[14] On MgO(001) the Au particles undergo strong modification upon annealing as seen by both the shift of the Au-related desorption peak to lower temperature and the smaller adsorption capacity indicated by the strong reduction of integrated area of the Au-related CO desorption (Figure 1a). This trend is well-known for oxide-supported Au clusters and is a direct result of particle sintering.[14] The situation is substantially different on the MgO_{hydr} sample (Figure 1b). Following annealing to 300 K the CO adsorption capacity of Au decreases, but the CO desorption temperature remains constant. Only after annealing to 500 K is the reduction of CO adsorption capacity accompanied by a decrease of the desorption temperature, which finally, after 650 K, reaches the same value (150 K) as for sintered gold clusters on MgO(001). After all annealing stages the CO adsorption capacity remains higher and can be directly correlated to an increased availability of CO adsorption sites on the Au/MgO_{hydr} sample.

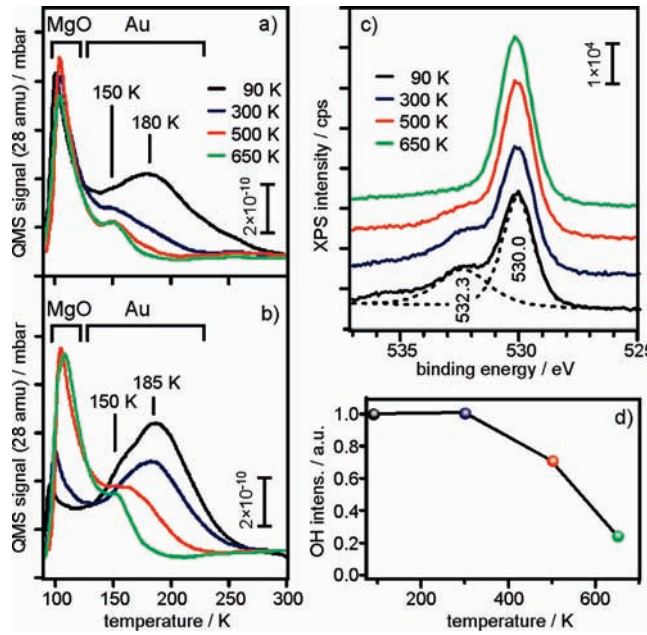

Figure 1. CO TPD spectra following exposure of CO at 90 K to 0.5 Å Au on (a) 20 ML MgO and (b) 20 ML MgO_{hydr} at different annealing temperatures. (c) O1s photoemission spectra collected from the sample shown in (b). (d) Normalized OH XPS intensity (532.3 eV) as a function of annealing temperature.

The TPD result suggests different sintering properties of Au particles on MgO_{hydr} surfaces as compared to nonhydroxylated ones. XPS measurements were performed to correlate this behavior with the hydroxylation state of the MgO_{hydr} surface. Figure 1c shows the O 1s photoemission spectra collected from 0.5 Å Au/MgO_{hydr} after the different annealing steps. The peak at 530.0 eV is assigned to the MgO

10.1021/ja100343m

substrate whereas the peak at 532.3 eV is assigned to surface hydroxyls.[15] The OH count rate, normalized to the intensity of the 90 K sample is shown in Figure 1d. Under conditions in which the MgO surface remains covered in OH (90 and 300 K) the corresponding desorption maximum (Figure 1b) from CO bound to Au particles remains stable at 185 K. After annealing to 500 and 650 K the OH concentration decreases due to H_2O desorption to about 70% and 25%, respectively, of the initial OH intensity (Figure 1d). The loss of hydroxyls is accompanied by a shift of the CO desorption peak, which finally reaches 150 K (Figure 1b), the same that is observed for nonhydroxylated MgO(001) (Figure 1a).

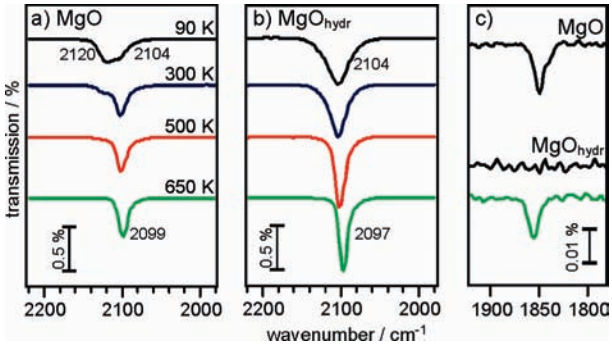

Figure 2. IR spectra of adsorbed CO for different annealing temperatures on 0.5 Å Au on (a) 20 ML MgO and (b) MgO_{hydr}. (c) Region surrounding the feature attributed to CO adsorbed on neutral Au atoms for 0.05 Å Au on MgO(001) and MgO_{hydr} (black traces) and after redepositing 0.05 Å Au on MgO_{hydr} following dehydroxylation at 650 K (green trace).

Figure 2 shows the IRAS spectra taken following exposure CO at 90 K for both 0.5 Å Au on (a) MgO(001) and (b) on MgO_{hydr} after various annealing steps. At all stages of the IRAS measurements the integrated intensity of the CO band from Au particles on MgO_{hydr} is higher than from that of MgO(001). The increased intensity, complementary to the TPD measurements presented in Figure 1a,b, further demonstrates that the number of CO adsorption sites on Au particles remains much higher on MgO_{hydr} at all annealing temperatures in this experiment. For the particles grown at 90 K two IR bands at 2120 cm^{-1} and 2104 cm^{-1} can be distinguished for Au on MgO(001), while a single broad band centered at 2104 cm^{-1} is present for Au on MgO_{hydr}. The latter can be assigned to CO adsorbed on LC, metallic sites on three-dimensional Au particles.[16] The 2120 cm^{-1} signal might arise from CO bound to either very small Au clusters[17] or slightly positively charged gold.[18] For annealing temperatures of 500 and 650 K, respectively, the signal around 2100 cm^{-1} is the only one present on both samples. The higher heterogeneity of CO adsorption sites on Au particles on MgO(001) evident from the 90 K spectra is related to different nucleation processes involving different nucleation sites on MgO(001) and MgO_{hydr} samples.

In order to shed more light on this aspect we performed IRAS measurements for a Au coverage of 0.05 Å, which is small enough to stabilize single Au atoms on MgO(001). Indeed, after adsorption of CO at 90 K an IR signal at ~1850 cm^{-1} (Figure 2c) is observed on the nonhydroxylated MgO(001) surface, indicating the presence of Au atoms adsorbed on MgO(001) terraces.[19] No additional IR signal is detected on MgO_{hydr} under these conditions. The inability for stabilization of single Au atoms on MgO_{hydr} is a direct consequence of the presence of surface OH groups, which block regular Au binding sites on MgO terraces, thereby enhancing diffusion and agglomeration into small clusters. These sites become available again after desorption of OH groups by dehydroxylation at 650 K (Figure 2c). With increasing temperature Au atoms diffuse rapidly across the MgO(001) surface and agglomerate into large particles exposing only a limited number of LC Au sites as seen by the shift of the CO desorption temperature and the reduction of the adsorption capacity in the TPD experiment (Figure 1a). By contrast, on the hydroxylated surface this process takes place only after significant reduction of the surface OH concentration (Figure 1b and 1c). Hydroxyl groups destabilize Au atoms on MgO at low temperature. However, they act to limit diffusion of small Au particles at intermediate temperatures, which is in close agreement with previous studies for Pb nucleation on MgO_{hydr}.[10c] Therefore, a high dispersion of small Au particles that possess a high density of LC adsorption sites is maintained on MgO_{hydr}.

In summary, hydroxyl groups are shown to strongly influence the nucleation and sintering behavior of gold on the MgO(001) surface. The stability of gold clusters toward sintering is enhanced on hydroxylated surfaces in a temperature range relevant for oxidation reactions on supported gold catalysts. In addition to particular Au support interactions that lead to stabilization of small, catalytically active Au particles on specific oxide supports, the surface hydroxyl coverage also influences the degree of particle dispersion by imposing a kinetic limitation on the thermodynamic driving force to form large, equilibrium shaped particles at higher annealing temperature.

Acknowledgment. We acknowledge the Alexander von Humboldt foundation (M.B.) and the Spanish Ministry of Science and Innovation (E.C.).

Supporting Information Available: Experimental details. This material is available free of charge via the Internet at http://pubs.acs.org.

References

(1) Haruta, M.; Tsubota, S.; Kobayashi, T.; Kageyama, H.; Genet, M. J.; Delmon, B. *J. Catal.* **1993**, *144*, 175.
(2) Valden, M.; Lai, X.; Goodman, D. W. *Science* **1998**, *281*, 1647.
(3) Boccuzzi, F.; Chiorino, A.; Manzoli, M.; Lu, P.; Akita, T.; Ichikawa, S.; Haruta, M. *J. Catal.* **2001**, *202*, 256.
(4) (a) Campbell, C. T. *Surf. Sci. Rep.* **1997**, *27*, 1. (b) Freund, H.-J. *Angew. Chem., Int. Ed.* **1997**, *36*, 452. (c) Henry, C. R. *Surf. Sci. Rep.* **1998**, *31*, 235. (d) Fu, Q.; Wagner, T. *Surf. Sci. Rep.* **2007**, *62*, 431.
(5) (a) Yulikov, M.; Sterrer, M.; Heyde, M.; Rust, H.-P.; Risse, T.; Freund, H.-J.; Pacchioni, G.; Scagnelli, A. *Phys. Rev. Lett.* **2006**, *96*, 146804. (b) Sterrer, M.; Yulikov, M.; Fischbach, E.; Heyde, M.; Rust, H.-P.; Pacchioni, G.; Risse, T.; Freund, H.-J. *Angew. Chem., Int. Ed.* **2006**, *45*, 2630.
(6) (a) Veith, G. M.; Lupini, A. R.; Dudney, N. J. *J. Phys. Chem. C* **2009**, *113*, 269. (b) Daniells, S. T.; Makkee, M.; Moulijn, J. A. *Catal. Lett.* **2005**, *100*, 39.
(7) Costello, C. K.; Kung, M. C.; Oh, H.-S.; Wang, Y.; Kung, H. H. *Appl. Catal., A* **2002**, *232*, 159.
(8) Cunningham, D. A. H.; Vogel, W.; Haruta, M. *Catal. Lett.* **1999**, *63*, 43.
(9) Qiao, B.; Zhang, J.; Liu, L.; Deng, Y. *Appl. Catal., A* **2008**, *340*, 220.
(10) (a) Libuda, J.; Frank, M.; Sandell, A.; Andersson, S.; Brühwiler, P. A.; Bäumer, M.; Mårtensson, N.; Freund, H.-J. *Surf. Sci.* **1997**, *384*, 106. (b) Jensen, M. C. R.; Venkataramani, K.; Helveg, S.; Clausen, B. S.; Reichling, M.; Besenbacher, F.; Lauritsen, J. V. *J. Phys. Chem. C* **2008**, *112*, 16953. (c) Starr, D. E.; Diaz, J. E.; Ranney, J. T.; Bald, D. J.; Nelen, L.; Ihm, H.; Campbell, C. T. *Surf. Sci.* **2002**, *515*, 13.
(11) Matthey, D.; Wang, J. G.; Wendt, S.; Matthiesen, J.; Schaub, R.; Laegsgaard, E.; Hammer, B.; Besenbacher, F. *Science* **2007**, *315*, 1692.
(12) Wu, T.; Kaden, W. E.; Anderson, S. L. *J. Phys. Chem. C* **2008**, *112*, 9006.
(13) Sterrer, M.; Risse, T.; Freund, H.-J. *Surf. Sci.* **2005**, *596*, 222.
(14) (a) Shaikhutdinov, Sh.K.; Meyer, R.; Naschitzki, M.; Bäumer, M.; Freund, H.-J. *Catal. Lett.* **2003**, *86*, 211. (b) Gross, E.; Asscher, M.; Lundwall, M.; Goodman, D. W. *J. Phys. Chem. C* **2007**, *111*, 16197.
(15) Liu, P.; Kendelewicz, T.; Brown, G. E.; Parks, G. A. *Surf. Sci.* **1998**, *412*−*413*, 287.
(16) (a) Bond, G. C.; Thompson, D. T. *Catal. Rev. Sci. Eng.* **1999**, *41*, 319. (b) Meyer, R.; Lemire, C.; Shaikhutdinov, Sh. K.; Freund, H.-J. *Gold Bull.* **2004**, *37*, 72.
(17) Lemire, C.; Meyer, R.; Shaikhutdinov, Sh.K.; Freund, H.-J. *Surf. Sci.* **2004**, *552*, 27.
(18) Boronat, M.; Concepción, P.; Corma, A. *J. Phys. Chem. C* **2009**, *113*, 16772.
(19) (a) Sterrer, M.; Yulikov, M.; Risse, T.; Freund, H.-J.; Carrasco, J.; Illas, F.; Di Valentin, C.; Giordano, L.; Pacchioni, G. *Angew. Chem., Int. Ed.* **2006**, *45*, 2633. (b) Yulikov, M.; Sterrer, M.; Risse, T.; Freund, H.-J. *Surf. Sci.* **2009**, *603*, 1622.

JA100343M